Applied Catalysis B: Environmental 343 (2024) 123487

Contents lists available at ScienceDirect

Applied Catalysis B: Environmental

journal homepage: www.elsevier.com/locate/apcatb

Co-existence of atomically dispersed Ru and Ce^{3+} sites is responsible for excellent low temperature N_2O reduction activity of Ru/CeO_2

Inhak Song [a], Yong Wang [a,b], János Szanyi [a,*], Konstantin Khivantsev [a,*]

[a] Institute for Integrated Catalysis, Pacific Northwest National Laboratory, Richland, WA 99352, United States
[b] Voiland School of Chemical Engineering and Bioengineering, Washington State University, Pullman, WA 99164, United States

ARTICLE INFO

Keywords:
Ruhenium
Rhodium
Ceria
Nitrous oxide reduction
Atomically dispersed catalyst

ABSTRACT

Nitrous oxide N_2O reduction is a big challenge due to high global warming potential of N_2O. (~300 times higher compared with CO_2). The best known catalysts, such as Rh/ceria, require relatively high temperatures for N_2O decomposition. Herein, we report that Ru/ceria catalysts with low Ru loading of ~0.25 wt% efficiently catalyze low temperature N_2O reduction by CO starting at 100 °C (full N_2O conversion below 200 °C) under industrially relevant flow rates and gas concentrations. This remarkable performance stems from maintaining isolated Ru cations even on reduced ceria surface and, simultaneously, the propensity of Ru to affect ceria surface to form labile surface oxygen thereby creating large number of oxygen vacancies (Ce^{3+} cations) in the presence of CO. In contrast, for Rh/CeO_2 catalysts with equivalent metal loading, the activity is much lower because atomically dispersed Rh sinters into metallic clusters at the onset reaction temperature (~200 °C): these clusters are much less effective than isolated single Ru ions, with lower Ce^{3+} concentration maintained on reduced Rh/CeO_2 catalyst. Our study highlights the benefits of gaining molecular-level insight into the dynamic nature of catalytically active sites under reaction conditions for preparing catalysts containing low loading of precious metals with unsurpassed low temperature activity.

1. Introduction

The recent oil-based energy crisis, global environmental pollution, and accelerating climate change are bringing the end of the current era of internal combustion engine much earlier than expected. Many automakers around the world are scaling back the development of new diesel engines and are moving the market in the transition period toward electric vehicles by maximizing the durability and efficiency of advanced gasoline combustion technologies [1,2]. Pd-, Pt-, and Rh-based modern three-way catalysts (TWC) are the pinnacle of the aftertreatment technology and have been steadily investigated and improved over the past several decades [3–6]. Unburned hydrocarbons and CO are oxidized by clustered, ensemble sites of Pd and Pt, and a dispersed small amount of Rh can reduce NOx. Dispersed cerium oxides stabilized with other rare earth metals on thermally stable alumina supports can temporarily store oxygen, thereby broadening the operating window of the catalysts under varying air/fuel ratios (λ) [7,8]. Nevertheless, one of the several remaining problems is the undesired formation of N_2O during TWC operation, which has 300 times higher greenhouse gas effect than carbon dioxide [9,10]. It is challenging to decompose N_2O with the conventional TWC catalysts.

The concept of atomically dispersed active sites, i.e., single atom catalysts (SAC) has received great attention recently, due to their catalytic properties that are often different from clusters/particles [11]. It has been reported that monoatomic metal cations, such as Pt, Rh, and Ru, are stably dispersed on the reducible support under oxidizing conditions due to strong M-O-Ce bonds [12–16]. These systems exhibit largely different catalytic behavior from typical metallic clusters. Unfortunately, most of the currently used *ex situ* analyses to prove single active sites have limitations under reaction conditions since the metal sites exhibit dynamic behavior affected by external variables such as reducing atmosphere and elevated temperatures. For example, Pd(II) ions dispersed in zeolites are readily clustered to metallic ensembles once they are exposed to water and CO even at ambient temperature [17–19]. The question arises here is whether a single active site can be retained on a reduced support even under a reducing atmosphere.

Thermal decomposition of N_2O typically requires rather high temperatures (>300 °C), so investigating a reduction route by utilizing abundant reductant contained in exhaust gas can be an efficient way for N_2O abatement [20–22]. In this study we discovered that a low loading

* Corresponding authors.
E-mail addresses: janos.szanyi@pnnl.gov (J. Szanyi), konstantin.khivantsev@pnnl.gov (K. Khivantsev).

https://doi.org/10.1016/j.apcatb.2023.123487
Received 31 July 2023; Received in revised form 1 November 2023; Accepted 6 November 2023
Available online 7 November 2023

of atomically dispersed Ru sites on the ceria support (~0.25 wt%) results in a catalyst that can reduce N_2O with CO at low temperatures starting at 100 °C and with full conversion below 200 °C under industrially relevant gas flows and concentrations of N_2O, outperforming previously described most efficient Rh/Ceria catalysts. We found that both Rh and Ru exist as atomically dispersed cation on the oxidized ceria surface, but Rh readily aggregates on the reduced ceria surface at ~200 ℃ (causing the onset of N_2O reduction activity), whereas Ru retains its dispersed state up to 300 °C in the presence of CO reductant. Simultaneously, the presence of Ru cations affects ceria surface leading to more labile surface oxygen which, in the presence of CO, forms a high concentration of surface Ce^{+3} sites (oxygen vacancies). Using reaction measurement and infra-red spectroscopy, we provide evidence that this difference between Rh and Ru supported on ceria is the main factor determining the N_2O decomposition activity at low temperatures. Our study provides methodology to synthesize highly active ceria-based catalysts for catalytic N_2O reduction.

2. Experimental methods

Cerium oxide was prepared by thermal decomposition of cerium (III) nitrate hexahydrate (99.9%, Sigma Aldrich). The precursor powder was placed in an alumina crucible and heated in a static furnace at 350 °C for 5 h under ambient air with a 1 °C/min ramp-up rate. The resulting yellowish solid was gently ground to a powder in mortar and further used as ceria support for platinum-group metals. Rh/ceria and Ru/ceria with 0.25 wt% Ru or Rh loading were prepared by incipient wetness impregnation method. Ruthenium(III) nitrosyl nitrate solution (1.5% metal, Alfa Aesar) and Rhodium(III) nitrate solution (10 wt%, Sigma Aldrich) was dissolved in a certain amount of evaporated water to make precursor solutions. Normally, about 1 g of ceria powder was dried in an oven at 70 °C for 1 h before impregnation. 250 μL of Rh or Ru precursor solution was slowly added, i.e. 10 μL at once by using pipet, to ceria powder with continuous mixing and mild grinding. The resulting powder was dried in an oven at 70 °C overnight, and subsequently calcined in air at 800 °C for 5 h with the ramp-up rate of 2 °C/min.

The in situ diffuse reflectance infra-red experiments were conducted in a commercial Harrick DRIFTS cell equipped with ZnSe window. The spectra were collected on Nicolet iS50 FT-IR (Thermo Fisher Scientific Co., USA) spectrometer with a liquid nitrogen-cooled MCT detector. Each spectrum was obtained as the average of 32 scans with 4 cm^{-1} resolutions. A background spectrum was recorded with KBr powder at temperatures where measurements were conducted. The space through which the IR beam passes on both sides of the reactor window was continuously purged with nitrogen to maintain a constant background. The sample holder inside DRIFTS cell was filled with α-alumina powder (Alfa Aesar) in every experiment. On top of α-alumina powder, a thin layer of Rh/ceria or Ru/ceria catalysts were spread and pressed firmly. Gas stream through the DRIFTS cell was controlled by mass flow controllers. Normally 0.03 g of powder was loaded in cell and the flow rate was adjusted to 50 mL/min. The outlet of the DRIFTS cell was connected to a quadrupole mass spectrometer (Hiden Analytical). The $m/z = 30$ fragment was tracked to measure N_2O concentration, which has ~30% relative intensity compared to main $m/z = 44$ signal. During ramping, DRIFTS spectra were continuously collected per every 30 s, while gas composition of the cell was continuously monitored with mass spectrometer.

The direct and CO-assisted catalytic N_2O decomposition was performed using a plug flow reactor system where the concentrations of reactants and products are quantified using a FTIR gas analyzer (MKS, Multigas 2030). The catalyst powders were sieved (180–250 μm) for the reaction, and loaded in a quartz reactor above a porous bed. Prior to reaction tests, the catalysts were pretreated in a flowing air (200 mL/min) for 30 min at 500 °C. The temperature programed reactions were performed under 670 ppm N_2O/N_2 and 1100 ppm CO/N_2 (when used) by ramping the reactor with 5 °C/min (GHSV: 225,000 $mL{\cdot}g^{-1}{\cdot}h^{-1}$). The kinetic dependences of N_2O decomposition were measured isothermally at 450 °C by varying N_2O concentration from 200 to 670 ppm. The kinetic dependences of N_2O reduction with CO were measured isothermally at 160 or 180 °C by varying N_2O concentration from 200 to 670 ppm or varying CO concentration from 200 to 1100 ppm. The measurements were performed under less than 20% N_2O conversion without any limiting reactants.

3. Results and discussions

3.1. N_2O decomposition over highly dispersed, ceria-supported Ru and Rh catalysts

Catalysts with 0.25 wt% Ru and Rh on ceria support were prepared by atom trapping following previously reported methods [23]. When these Ru/ceria or Rh/ceria catalysts are exposed to an oxidizing atmosphere at high temperatures, the oxidized RuO_x or RhO_x are located on the most stable sites on the ceria surfaces, which is the driving force to create and stabilize atomically dispersed sites [13]. First, the activities of direct N_2O decomposition over both catalysts were compared (Fig. 1). Neither catalyst decompose N_2O up to 350 °C, and they start to decompose N_2O only when the temperature exceeds 350 °C. Even at 500 °C, however, both catalysts show low N_2O conversion of around 20%. Although small amounts of isolated PGM ions do not promote the reduction of N_2O, they are known to help the reduction of ceria surface to form oxygen vacancies [2,13]. The question is whether these oxygen vacancies created on the ceria surface can decompose N_2O. We tested the N_2O decomposition activity after reducing both catalysts in a flow of 1100 ppm CO at 200 °C (Fig. 1). Interestingly, the 0.25Ru/ceria catalyst shows notable transient N_2O reduction activity between 150 and 250 °C. Above 300 °C the activity of this catalyst was identical to that of the non-reduced catalyst indicating that oxygen vacancies created by CO treatment were consumed by reacting with N_2O, and it was unable to

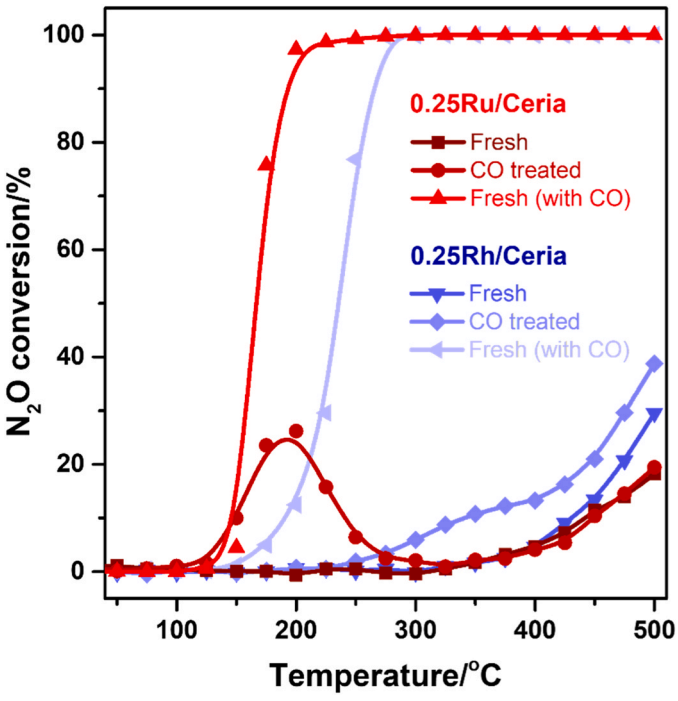

Fig. 1. Catalytic conversion of N_2O with 0.25Ru/ceria and 0.25Rh/ceria catalysts. The activity was measured after dehydration at 200 °C (Fresh) and reduction with CO at 200 °C for 1 h (CO treated). The activity of N_2O decomposition with CO (Fresh (with CO)) was also tested. The feed gas contains 670 ppm N_2O, 1100 ppm CO (when used) balance with N_2. (GHSV: 225,000 $mL{\cdot}g^{-1}{\cdot}h^{-1}$).

sustain its activity after the oxygen vacancies were filled by the oxygen atoms originating from the decomposition of N_2O. Unlike Ru/ceria, Rh/ceria shows no activity below 250 °C. The transient N_2O consumption induced by CO treatment begins to appear above 250 °C and continues up to 500 °C. Such difference between Rh and Ru is more clearly observed when both N_2O and CO are introduced into the reactor. Under the slightly rich conditions applied reduction of N_2O with CO can take place. Over the Ru/Ceria catalyst, N_2O decomposition starts above ~120 °C and reaches 100% N_2O conversion ~200 °C. In contrast, the Rh/ceria catalyst shows activity only starting at ~180 °C and does not reach 100% N_2O conversion until 300 °C. Obviously, Ru/Ceria has a significantly higher N_2O reduction activity with CO than Rh/ceria catalyst. This is a notable finding considering that Rh/CeO_2 has been regarded as the best N_2O decomposition catalysts [20]. We further tested 0.25 wt% Ru supported on reducible and partially reducible supports (titania and zirconia) for N_2O decomposition under identical conditions as in Fig. 1 (Figs S2, S3). Notably, their activity was significantly lower than that of Ru/CeO_2 with no low-temperature activity observed for Rh/TiO_2 and lower low-temperature activity observed for Rh/ZrO_2.

To further investigate the N_2O decomposition with pre-formed oxygen vacancies on Ru/ceria catalyst, the reaction was conducted after CO treatment at various temperatures from 100° to 400°C (Fig. 2). The amount of reacted N_2O is very small after 100 °C reduction since the degree of reduction is limited at this low temperature. With increasing reduction temperature N_2O conversion is expected to increase. However, the amount of reacted N_2O is maximized after 200 °C reduction and then gradually decreases after 300 and 400 °C reduction. Note that there is no decrease in surface area for this sample since it has already been oxidized at 800 °C. This is a very important observation indicating that not all oxygen vacancies on the ceria surface can react with N_2O. The decreasing amount of transient N_2O consumption above 300 °C can originate from clustering of metallic Ru during CO treatment. The formation of metallic Ru after reduction is evidenced by the increased N_2O decomposition activity at 500 °C with increasing pre-reduction temperature, revealing that metallic Ru nanoparticles are the active species for direct N_2O decomposition at high temperature. Thus, even if the Ru/ceria surface is reduced by CO and oxygen vacancies are created, single Ru or metallic Ru must exist near oxygen vacancies for them to react with N_2O. That is, N_2O does not directly react with surface oxygen vacancies but requires Ru sites. This hypothesis explains well why the amount of N_2O consumption is maximum at 200 °C, not 400 °C. To prove this, we created oxygen vacancies on pure ceria without Ru by H_2 reduction treatment at 500 °C and tested it under the same reaction condition (Fig. 2). Correspondingly, reduced ceria without Ru does not react with N_2O below 400 °C. At high temperature reductive treatment, reduction of ceria surface can occur with the formation of Ce^{+3} and oxygen vacancies that are the active sites for NxOy reduction at higher temperature as shown spectroscopically in our recent work, consistent with catalytic data for bare ceria in Fig. 2 [29].

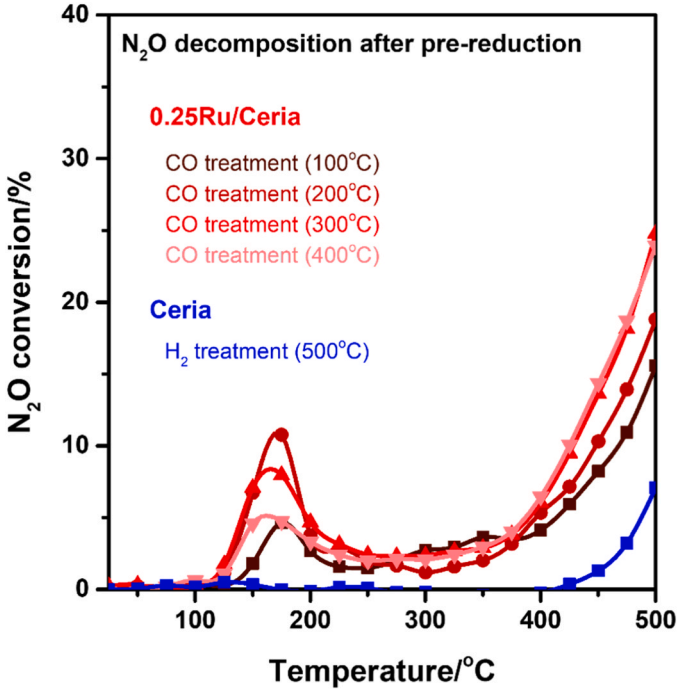

Fig. 2. Catalytic conversion of N_2O with 0.25Ru/Ceria after reductive treatment at different temperatures. The activity of 0.25Ru/ceria was measured after pre-reduction with CO at 100–400 °C for 1 h. The activity of pure ceria was measured after reduction with H_2 at 500 °C for 1 h. The feed gas contains 670 ppm N_2O, 1100 ppm CO (when used) balance with N_2.

3.2. Observation of surface reduction by CO treatment

We have shown above (Fig. 1) that mild CO treatment at 200 °C enabled Ru/ceria to decompose N_2O below 150 °C, while the same reductive treatment had no such effect on the performance of Rh/Ceria catalyst. The results in Fig. 1 suggests that reduction of the CeO_2-supported metal catalysts by CO at 200 °C creates active sites for the decomposition of N_2O. However, it is also evident from these results that the active sites for N_2O decomposition are not only the defect sites on the CeO_2 support, as the onset of N_2O decomposition temperature strongly depends on the nature of the metal (~120 °C for Ru/Ceria and ~200 °C for Rh/Ceria). These observations are in agreement with our inference from Fig. 2 that N_2O decomposition over these catalysts requires the participation of both the metal sites and Ce^{+3} sites (oxygen vacancies) on the ceria support. The different extent of reduction of the two supported metal catalysts by CO at 200 °C is evident from the results shown in Fig. 3a: the amount of CO consumed by these two materials during the reduction is vastly different. Both catalysts consume significant amounts of CO during the first 15 min, and the outlet CO level returns to the bypass level after 40 min CO exposure. The amount of CO consumed by the Ru/ceria catalyst is ~35% higher (CO/Ru~12) than that by the Rh/ceria (CO/Rh~9) [24]. The larger amount of CO consumed by the Ru/Ceria catalysts, in comparison to that over the Rh/Ceria, during this process is in line with the larger amount of N_2O consumption during the temperature programmed reaction over the CO-reduced Ru/ceria catalyst (Fig. 1). Parallel to these flow reactor studies we also conducted in situ DRIFTS experiments to follow the changes occurring on the surfaces of these catalysts during the CO treatment at 200 °C. The series of DRIFT spectra collected during the 20 min CO exposure of the 0.25Ru/Ceria catalyst exhibit a wealth of absorption bands with identifiable IR features (Fig. 3b). IR bands observed at the early stage of CO exposure represent mostly di- and tri-carbonyl species bound to cationic Ru^{2+} sites [14]. The two most intense, sharp IR features between 1900 and 2100 cm^{-1} encompass the features of both tri- and di-carbonyl species on oxidized, highly (atomically) dispersed Ru cations, which is consistent with the results from our recent work [14]. Tri-carbonyls on Ru^{2+} ions should have three distinct vibrational bands, in the spectral series of Fig. 3b they are located at 2122, 2064 and 2054 cm^{-1} (although, this broad high frequency band also contains contributions from di-carbonyl species). The low frequency portion of the signature vibration of di-carbonyl species is observed between 1950 and 2040 cm^{-1}, clearly showing the formation of more than one type of di-carbonyl species, probably associated with Ru cations in different coordination environments on the Ceria surface. These doublets are strong evidence that Ru cations are atomically dispersed on ceria surface, because these bands severely lose their intensities and shift to lower wavenumber after reduction treatment under H_2, which removes oxygen from Ru cations and reducing them to metal (Fig. S1). As the IR features representing di- and tri-carbonyl species adsorbed onto cationic Ru sites reach

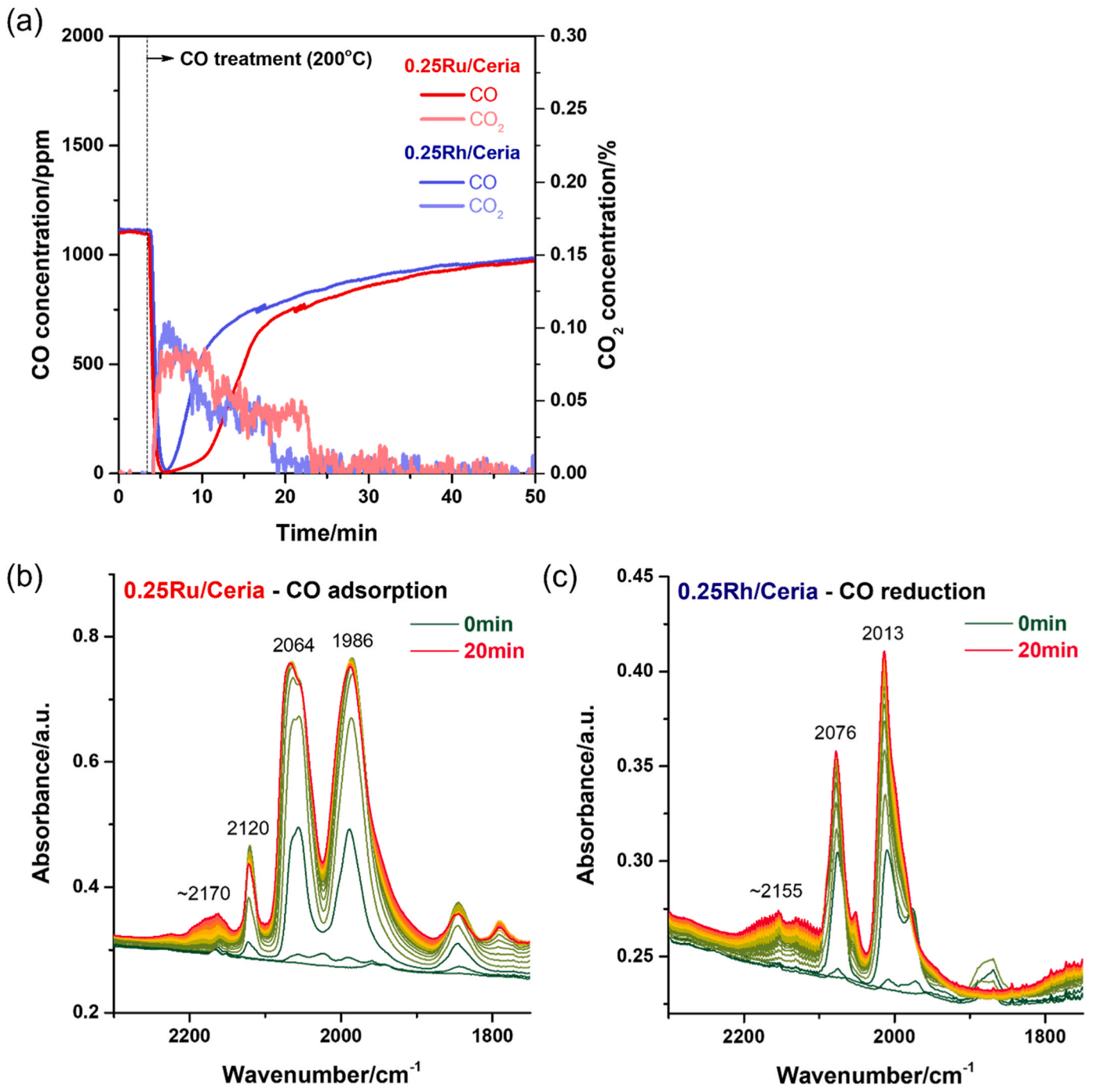

Fig. 3. (a) Profiles of CO and CO_2 concentrations during CO treatment at 200 °C for 0.25Ru/ceria and 0.25Rh/ceria catalysts in plug flow reactor. Series of DRIFTS spectra (per 30 s) obtained at 200 °C while flowing 1000 ppm CO/He on (b) 0.25Ru/ceria and (c) 0.25Rh/ceria catalyst. Before flowing CO, the sample was dehydrated at 500 °C for 30 min under 3% O_2/He.

saturation, a broad band between 2200 and 2100 cm^{-1} gradually gains intensity. This band can be assigned to the forbidden $^2F_{5/2} \rightarrow {}^2F_{7/2}$ electronic transition of Ce^{3+} ions [25], indicating that ceria surface is gradually being reduced with CO. In summary, after the 20 min exposure of the Ru/Ceria catalyst to CO, Ru is present in highly (atomically) dispersed cationic form while the CeO_2 support contains oxygen vacancies.

For 0.25Rh/Ceria (Fig. 3c), dicarbonyl bands centered at 2076 and 2013 cm^{-1} similarly form on the cationic Rh^{1+} sites in the first few minutes [7,13]. The broad band (2200 and 2100 cm^{-1}) arises from electronic transition on Ce^{3+} ions also gradually appear showing the reduction of the ceria surface. Interestingly, a new band gradually forms near 2050 cm^{-1} as the ceria surface is reduced. The band is consistent with CO adsorbed on Rh clusters. That is, as the ceria surface gets more reduced, Rh ions get reduced and agglomerate into Rh clusters. We infer that the onset of catalytic activity for N_2O reduction with CO at this temperature (~200 °C) is consistent with metallic Rh cluster formation. Activity remains relatively low because only a fraction of Rh gets reduced at this temperature: IR data provide evidence that a significant fraction of Rh remains in an oxidized + 1 state when coordinated with CO molecules, forming typical $Rh(I)(CO)_2$ moiety. As will be mentioned later, the clustering of reduced Rh sites can be accelerated under the

condition when CO and N_2O coexist.

3.3. *In situ DRIFTS-MS and kinetic investigation of N_2O reduction with CO*

The reaction between N_2O and CO over Ru and Rh on ceria was monitored with increasing temperature by using in situ DRIFTS-MS (Fig. 4). The catalysts were pretreated with CO at 200 °C before starting the reaction. Similar to the reaction results above, the decomposition of N_2O on Ru/Ceria catalyst starts around 100 °C. Di- (with small amount of tri-) carbonyl adsorbed on cationic Ru (2057 and 1985 cm^{-1}) also stably present up to this temperature without any change in intensity. This shows that the reduction of N_2O with CO at this temperature (150–200 °C) occurs on highly dispersed Ru sites. In the meantime, dicarbonyl starts to shift to a lower wavenumber (2028 and 1960 cm^{-1}) above 300 °C due to the reduction of cationic Ru sites and formation of Ru clusters. Some of the reduced Ru begin to aggregate into metallic clusters, evidenced by growing bridging monocarbonyl bands located at 1900 cm^{-1}. For Rh/ceria catalyst (Fig. 4d-f), the decomposition of N_2O does not occur until 200 °C similar to the reaction results. Notably, the IR bands of dicarbonyl on cationic Rh^{+1} (2085 and 2018 cm^{-1}) rapidly decreases above 100 °C accompanied by the gradual growth of the bridging CO band near ~1862 cm^{-1}. Such observation suggests that dispersed Rh sites are much easily reduced than dispersed Ru sites, and also Rh tends to aggregate on the pre-reduced ceria surface.

Kinetic studies were conducted to confirm whether this different phenomenon of Rh and Ru on reduced ceria surface can affect the reaction pathway (Fig. 5). Under direct N_2O decomposition conditions without CO, both catalysts have a similar reaction order to N_2O of about 0.6. This is because the reaction rate increases in proportion to the N_2O partial pressure due to the weak interaction between N_2O and the catalyst surface [22]. During N_2O reduction with CO at low temperatures, Ru and Rh catalysts show largely different kinetic behavior. The reaction order of both N_2O and CO on the Ru catalyst is close to zero, indicating that the reaction proceeds in a similar pathway to the Langmuir-Hinshelwood kinetics. In other words, surface oxygen vacancies induced by reduction with CO reacts with weakly adsorbed N_2O on the surface. On the other hand, the reaction order of CO on Rh catalyst has been measured to be a negative value while the reaction order of N_2O has a positive value. It is known that such phenomenon is observed when CO adsorbs too strongly on metallic clusters preventing other reactants from accessing the active sites [26,27]. Unlike Ru sites that are maintained as isolated sites under reaction conditions, Rh easily forms clusters on the reduced ceria surface. Furthermore, what we can learn from this observation is that atomically dispersed Ru sites are required for N_2O to react with oxygen vacancy at low temperatures because they still catalyze reaction as CO-coordinated states unlike rhodium clusters [27,28]. Both Ru and Rh can be atomically dispersed on the oxidized ceria surface, but the fact that Ru can retain dispersed state even on reduced ceria surface helps the reaction to occur at much lower temperature. Simultaneously, the presence of Ru^{+2} ions affects ceria surface leading to more labile oxygen that can react with CO,

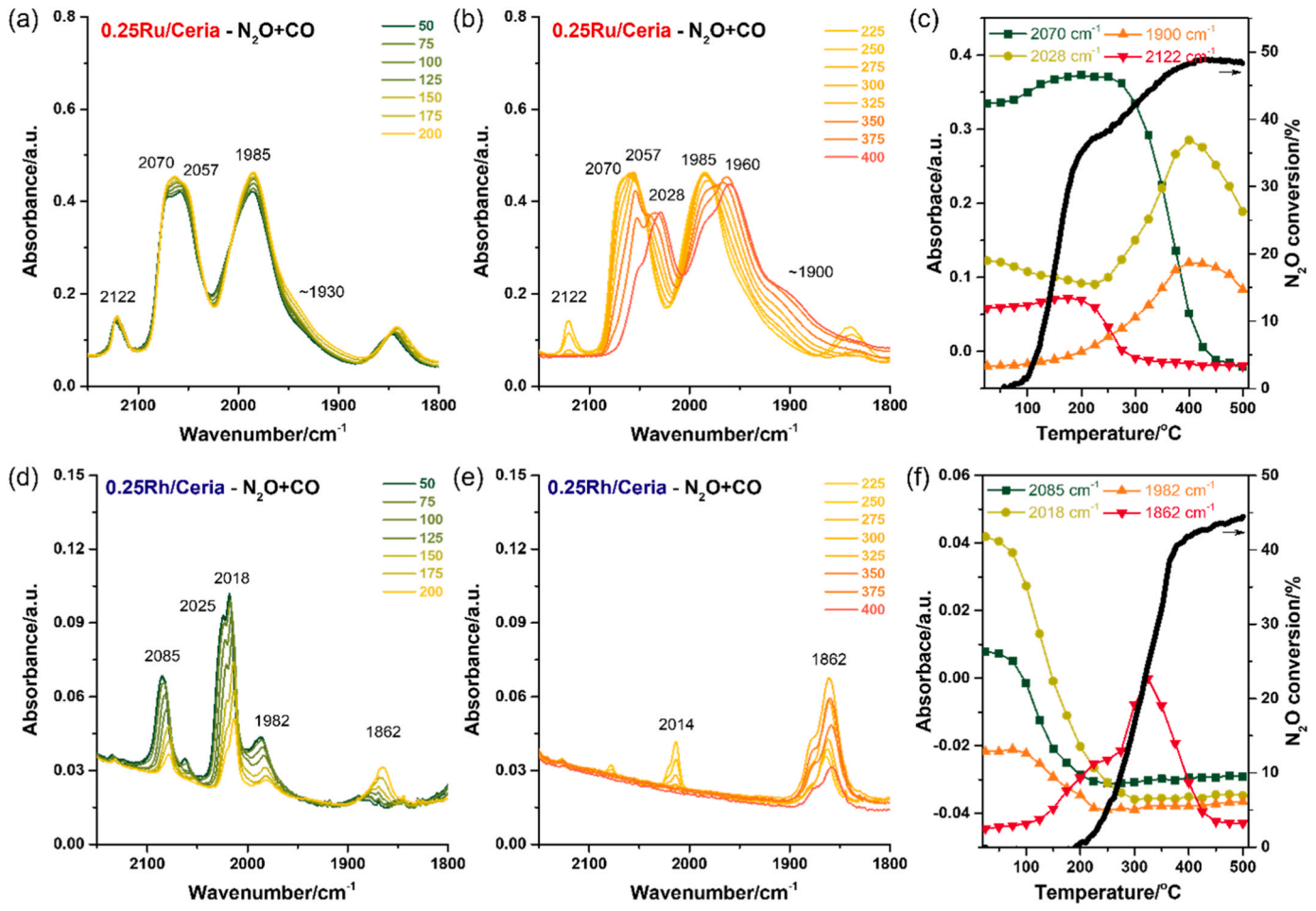

Fig. 4. The N_2O reduction with CO on (a-c) 0.25Ru/Ceria and (d-f) 0.25Rh/Ceria were investigated by DRIFTS-MS. Series of DRIFTS spectra (per 25 °C) obtained during heating from 25° to 200°C and 200–400 °C while flowing 800 ppm N_2O + 1000 ppm CO/He were plotted, respectively. Before flowing N_2O+CO, the catalyst was pretreated with 1000 ppm CO/He at 200 °C for 1 h. The change in various IR band intensities and N_2O conversion measured by MS with increasing temperature were also compared.

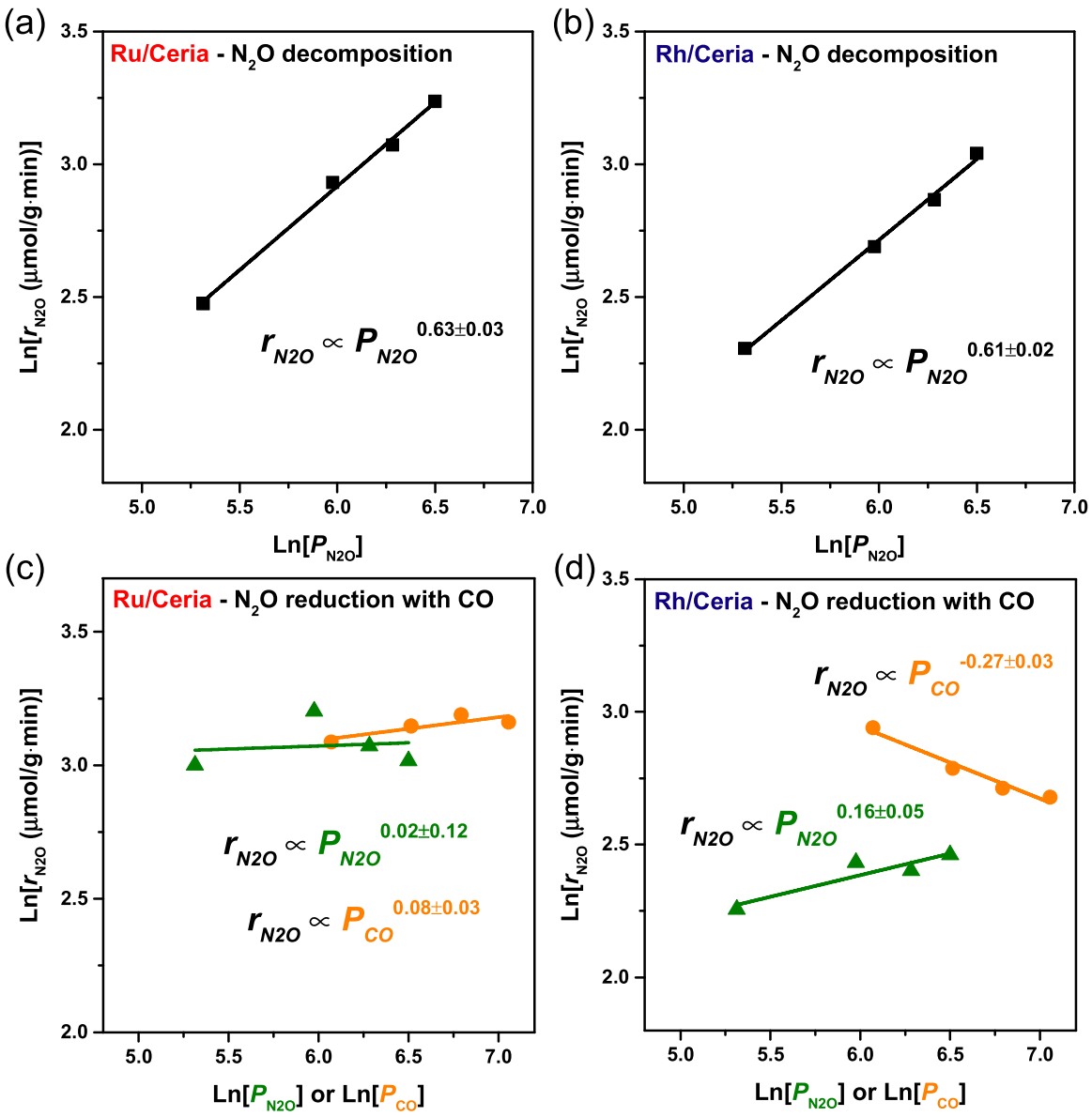

Fig. 5. (a, b) Logarithm of the reaction rate of N_2O decomposition on Ru/ceria and Rh/ceria catalysts at 450 °C as a function of logarithm of P_{N2O} and P_{CO}. (c, d) Logarithm of the reaction rate of N_2O reduction with CO on Ru/ceria (160 °C) and Rh/ceria (180 °C) catalysts as a function of logarithm of P_{N2O} and P_{CO}.

forming a significant fraction of oxygen vacancies on the surface of ceria. Furthermore, the isolated Ru ions are maintained on the reduced ceria surface, ensuring effective reaction with N_2O, restoring Ru-O-Ce, and completing the catalytic cycle.

4. Conclusions

We synthesized and investigated atomically dispersed Rh and Ru cations on ceria catalysts for catalytic N_2O decomposition. Excellent low temperature activity was observed for N_2O reduction on Ru/ceria catalyst even at low Ru loading. Ru/Ceria exhibits activity already at ~100 °C and fully converts N_2O at ~200 °C whereas Rh/Ceria starts to convert N_2O only at ~200 °C achieving full conversion at 300 °C. Both metals are able to induce the reduction of ceria surface at a mild temperature ~ 200 °C, but the oxygen vacancy formed in this process could readily react with N_2O on only reduced Ru/ceria. This is due to unstable nature of single Rh sites on reduced ceria surface that agglomerate into partially CO covered metallic clusters at low temperature inhibiting the reaction of N_2O with oxygen vacancy on the ceria surface. In contrast, single Ru site remained stable up to 300 °C in an isolated state after ceria was reduced, implying that co-existence of atomically dispersed Ru and Ce^{3+} sites are critical for N_2O reduction at low temperature.

CRediT authorship contribution statement

Inhak Song: Investigation; Data curation; Formal analysis; Methodology; Writing – original draft, Writing – review & editing. **Yong Wang:** Funding acquisition; Writing – original draft. **Janos Szanyi:** Funding acquisition; Data curation; Writing – original draft, Writing – review & editing. **Konstantin Khivantsev**: Conceptualization; Methodology; Data curation; Formal analysis; Project administration; Supervision; investigation; Writing – original draft, Writing – review & editing.

Declaration of Competing Interest

The authors declare that they have no known competing financial interests or personal relationships that could have appeared to influence

the work reported in this paper.

Data Availability

Data will be made available on request.

Acknowledgments

The authors gratefully acknowledge the US Department of Energy (DOE), Energy Efficiency and Renewable Energy, Vehicle Technologies Office for the support of this work. The research described in this paper was performed in the Environmental Molecular Sciences Laboratory (EMSL), a national scientific user facility sponsored by the DOE's Office of Biological and Environmental Research and located at Pacific Northwest National Laboratory (PNNL). PNNL is operated for the US DOE by Battelle.

Dr. Inhak Song's present address is Department of Energy Environment Policy and Technology, Graduate School of Energy and Environment (KU-KIST Green School), Korea University, Seoul 02841, Republic of Korea

Appendix A. Supporting information

Supplementary data associated with this article can be found in the online version at doi:10.1016/j.apcatb.2023.123487.

References

[1] J. Demuynck, P. Mendoza Villafuerte, D. Bosteels, G. Randlshofer, Ultra-low emissions of a 48V mild-hybrid gasoline vehicle with advanced emission control technologies and system control, SAE Tech. Pap. (2021) 24–0070.
[2] J. Lee, Y. Kim, S. Hwang, G.S. Hong, E. Lee, H. Lee, C. Jeong, C.H. Kim, J.S. Yoo, D. H. Kim, Toward gasoline vehicles with zero harmful emissions by storing NO at Pd nanoparticle–CeO2 interface during the cold-start period, Chem. Catal. (2022).
[3] A.K. Datye, M. Votsmeier, Opportunities and challenges in the development of advanced materials for emission control catalysts, Nat. Mater. 20 (8) (2021) 1049–1059.
[4] S. Rood, S. Eslava, A. Manigrasso, C. Bannister, Recent advances in gasoline three-way catalyst formulation: a review, Proc. Inst. Mech. Eng., Part D: J. Automob. Eng. 234 (4) (2020) 936–949.
[5] K. Khivantsev, H. Pham, M. Engelhard, H. Aleksandrov, X. Li, J. Tian, I. Koleva, X. Wei, Y. Sun, P. Tran, Dramatic improvement of NO reduction activity via reversible re-dispersion of CeO2 nanoparticles into Ce+ 3 atoms on alumina under high temperature reactive treatment, Chemrxiv (2022), https://doi.org/10.26434/chemrxiv-2021-spcd9-v2.
[6] H. Asakura, S. Hosokawa, T. Ina, K. Kato, K. Nitta, K. Uera, T. Uruga, H. Miura, T. Shishido, J. Ohyama, Dynamic behavior of Rh species in Rh/Al2O3 model catalyst during three-way catalytic reaction: an operando X-ray absorption spectroscopy study, J. Am. Chem. Soc. 140 (1) (2018) 176–184.
[7] M. Shelef, G. Graham, Why rhodium in automotive three-way catalysts? Catal. Rev. 36 (3) (1994) 433–457.
[8] J. Kim, Y. Kim, M.H. Wiebenga, S.H. Oh, D.H. Kim, Oxidation of C3H8, iso-C5H12 and C3H6 under near-stoichiometric and fuel-lean conditions over aged Pt–Pd/Al2O3 catalysts with different Pt: Pd ratios, Appl. Catal. B: Environ. 251 (2019) 283–294.
[9] R. Wunsch, C. Schön, M. Frey, D. Tran, S. Proske, T. Wandrey, M. Kalogirou, J. Schäffner, Detailed experimental investigation of the NOx reaction pathways of three-way catalysts with focus on intermediate reactions of NH3 and N2O, Appl. Catal. B: Environ. 272 (2020), 118937.
[10] P. Nevalainen, N.M. Kinnunen, A. Kirveslahti, K. Kallinen, T. Maunula, M. Keenan, M. Suvanto, Formation of NH3 and N2O in a modern natural gas three-way catalyst designed for heavy-duty vehicles: the effects of simulated exhaust gas composition and ageing, Appl. Catal. A: Gen. 552 (2018) 30–37.
[11] R. Lang, X. Du, Y. Huang, X. Jiang, Q. Zhang, Y. Guo, K. Liu, B. Qiao, A. Wang, T. Zhang, Single-atom catalysts based on the metal–oxide interaction, Chem. Rev. 120 (21) (2020) 11986–12043.
[12] J. Jones, H. Xiong, A.T. DeLaRiva, E.J. Peterson, H. Pham, S.R. Challa, G. Qi, S. Oh, M.H. Wiebenga, X.I. Pereira Hernández, Thermally stable single-atom platinum-on-ceria catalysts via atom trapping, Science 353 (6295) (2016) 150–154.
[13] K. Khivantsev, C.G. Vargas, J. Tian, L. Kovarik, N.R. Jaegers, J. Szanyi, Y. Wang, Economizing on precious metals in three-way catalysts: thermally stable and highly active single-atom rhodium on ceria for NO abatement under dry and industrially relevant conditions, Angew. Chem. Int. Ed. 60 (1) (2021) 391–398.
[14] K. Khivantsev, N.R. Jaegers, H.A. Aleksandrov, I. Song, X.I. Pereira-Hernandez, M. H. Engelhard, J. Tian, L. Chen, D. Motta Meira, L. Kovarik, Single Ru (II) ions on ceria as a highly active catalyst for abatement of NO, J. Am. Chem. Soc. 145 (9) (2023) 5029–5040.
[15] I. Song, J. Szanyi, Y. Wang, K. Khivantsev, Understanding reactivity and stability of rhodium supported on different ceria facets in catalytic NO reduction and CO/hydrocarbon oxidation reactions, Chemrxiv (2023), https://doi.org/10.26434/chemrxiv-2023-9ldvr.
[16] J. Lee, Y. Ryou, X. Chan, T.J. Kim, D.H. Kim, How Pt interacts with CeO2 under the reducing and oxidizing environments at elevated temperature: the origin of improved thermal stability of Pt/CeO2 compared to CeO2, J. Phys. Chem. C. 120 (45) (2016) 25870–25879.
[17] I. Song, K. Khivantsev, Y. Wang, J. Szanyi, Elucidating the role of CO in the NO storage mechanism on Pd/SSZ-13 with *in Situ* DRIFTS, J. Phys. Chem. C. 126 (3) (2022) 1439–1449.
[18] R.P. Zelinsky, D.P. Dean, C.J. Breckner, S. Marino, J.T. Miller, W.S. Epling, Pd/BEA hydrocarbon traps: effect of hydrothermal aging on trapping properties and Pd speciation, Appl. Catal. B: Environ. (2022), 121938.
[19] I. Song, I.Z. Koleva, H.A. Aleksandrov, L. Chen, J. Heo, D. Li, Y. Wang, J. Szanyi, K. Khivantsev, Ultra small Pd clusters in FER zeolite alleviate CO poisoning for effective low temperature carbon monoxide oxidation, Chemrxiv (2023), https://doi.org/10.26434/chemrxiv-2023-6cwhw.
[20] S. Parres-Esclapez, M. Illán-Gómez, C.S.-M. De Lecea, A. Bueno-López, On the importance of the catalyst redox properties in the N2O decomposition over alumina and ceria supported Rh, Pd and Pt, Appl. Catal. B: Environ. 96 (3–4) (2010) 370–378.
[21] J. Pérez-Ramírez, M.S. Kumar, A. Brückner, Reduction of N2O with CO over FeMFI zeolites: influence of the preparation method on the iron species and catalytic behavior, J. Catal. 223 (1) (2004) 13–27.
[22] F. Lin, T. Andana, Y. Wu, J. Szanyi, Y. Wang, F. Gao, Catalytic site requirements for N2O decomposition on Cu-, Co-, and Fe-SSZ-13 zeolites, J. Catal. 401 (2021) 70–80.
[23] R. Alcala, A. DeLaRiva, E.J. Peterson, A. Benavidez, C.E. Garcia-Vargas, D. Jiang, X. I. Pereira-Hernández, H.H. Brongersma, R. ter Veen, J. Stanėk, Atomically dispersed dopants for stabilizing ceria surface area, Appl. Catal. B: Environ. 284 (2021), 119722.
[24] Y. Guo, S. Mei, K. Yuan, D.-J. Wang, H.-C. Liu, C.-H. Yan, Y.-W. Zhang, Low-temperature CO_2 methanation over CeO2-supported Ru single atoms, nanoclusters, and nanoparticles competitively tuned by strong metal–support interactions and H-spillover effect, ACS Catal. 8 (7) (2018) 6203–6215.
[25] M.Y. Mihaylov, E.Z. Ivanova, G.N. Vayssilov, K.I. Hadjiivanov, Revisiting ceria-NOx interaction: FTIR studies, Catal. Today 357 (2020) 613–620.
[26] M. Shelef, R.W. McCabe, Twenty-five years after introduction of automotive catalysts: what next? Catal. Today 62 (1) (2000) 35–50.
[27] J. Liu, F.R. Lucci, M. Yang, S. Lee, M.D. Marcinkowski, A.J. Therrien, C. T. Williams, E.C.H. Sykes, M. Flytzani-Stephanopoulos, Tackling CO poisoning with single-atom alloy catalysts, J. Am. Chem. Soc. 138 (20) (2016) 6396–6399.
[28] H.C. Kwon, M. Kim, J.-P. Grote, S.J. Cho, M.W. Chung, H. Kim, D.H. Won, A. R. Zeradjanin, K.J. Mayrhofer, M. Choi, Carbon monoxide as a promoter of atomically dispersed platinum catalyst in electrochemical hydrogen evolution reaction, J. Am. Chem. Soc. 140 (47) (2018) 16198–16205.
[29] K. Khivantsev, et al., Transforming CeO2 nanoparticles into ultra small ceria clusters on alumina enhances catalytic activity, ChemRxiv (2023), https://doi.org/10.26434/chemrxiv-2021-spcd9-v3.